NINA DEWI OKTAVIYANTI _ <nina_dewi@staff.ubaya.ac.id>

[IJCC] Editor Decision

1 message

ijcc@chemoprev.org <ijcc@chemoprev.org> Tue, May 12, 2026 at 1:55 PM
To: nina_dewi@staff.ubaya.ac.id

Dear Mrs. Nina Dewi Oktaviyanti,

We have reached a decision regarding your submission to Indonesian Journal of Cancer Chemoprevention, "Molegro Virtual Docker-Based Prediction of Rhodomyrtus tomentosa Metabolites Targeting Ribonucleotide Reductase as Potencial Anticancer Agents".

Our decision is to: Accept Submission

Prof. Adam Hermawan
Faculty of Pharmacy, Universitas Gadjah Mada
adam_apt@ugm.ac.id

IJCC

by Nina Dewi Oktaviyanti

Submission date: 04-Jun-2026 11:11AM (UTC+0700)
Submission ID: 2976061381
File name: 558-2337-3-ED.pdf (676.13K)
Word count: 6766
Character count: 39872

Molegro Virtual Docker-Based Prediction of *Rhodomyrtus tomentosa* Metabolites Targeting Ribonucleotide Reductase as Potential Anticancer Agents

Iman Nurjaman[1], Dini Kesuma[2], Tegar Achsendo Yuniarta[2], Nina Dewi Oktaviyanti[3*]

[1] Master's Degree Program in Industrial Pharmacy, Faculty of Pharmacy, University of Surabaya, Surabaya, Indonesia

[2] Department of Drug Discovery and Development, Faculty of Pharmacy, University of Surabaya, Surabaya, Indonesia

[3] Department of Pharmaceutical Manufacturing, Faculty of Pharmacy, University of Surabaya, Surabaya, Indonesia

*Corresponding Author. Email: nina_dewi@staff.ubaya.ac.id

Telp: +62 312981110

Abstract

The increasing number of cancer cases has prompted the search for new drug candidates from natural ingredients, particularly plant-derived compounds considered safer and more effective. *Rhodomyrtus tomentosa* (Aiton) Hassk. contains various metabolites responsible for various biological activities. This study aimed to predict the anticancer potential of *R. tomentosa* metabolites against the *Ribonucleotide Reductase* (RNR) enzyme using an in silico approach. The RNR protein structure (PDB ID: 2WGH) was obtained from the RCSB Protein Data Bank. Molecular docking was performed on 25 compounds previously reported in the literature as metabolites of *R. tomentosa* using Molegro Virtual Docker (MVD) version 7.0 to evaluate ligand-receptor binding affinity based on MolDock Score values using a validated docking protocol (RMSD $\leq$ 2.0 Å), followed by interaction analysis and pharmacokinetic evaluation using ADMET parameters. The results indicated that most compounds exhibited favorable binding affinities toward RNR, as reflected by negative MolDock Score values. Rhodomyrtosone B (−137.144 kcal/mol) showed the best binding affinity, followed by Malvidin-3-glucoside (−135.173 kcal/mol), Delphinidin-3-galactoside (-132.359 kcal/mol), Rhodomyrtosone I (−130.004 kcal/mol), and Cyanidin-3-galactoside (-127.741 kcal/mol). Interaction analysis revealed stable interactions with key amino acid residues (Arg256, Asp226, and Ser269) through hydrogen bonding, hydrophobic, and electrostatic interactions. ADMET analysis indicated variability in pharmacokinetic properties, including absorption, distribution, metabolism, and toxicity. In conclusion, Rhodomyrtosone B has potential as a natural product-based anticancer agent targeting RNR, providing a basis for further in vitro and in vivo studies.

Keywords: Anticancer; *Rhodomyrtus tomentosa*; Molecular Docking; *Ribonucleotide Reductase*; In Silico

Introduction

Cancer is one of the leading causes of death worldwide and remains a growing global health problem (Ferlay, et al., 2024). Data from the Global Cancer Observatory (GLOBOCAN) indicate that in 2022 there were more than 400,000 new cancer cases in Indonesia. The high incidence of cancer, together with the limitations of current therapies, drives the need for the development of new drug candidates that are more effective, selective, and associated with minimal side effects. Several conventional cancer therapies such as chemotherapy, radiotherapy, immunotherapy, and molecular targeted therapy still have limitations, including high toxicity, high costs, and the emergence of drug resistance such as multidrug resistance (MDR) (Gu, et al., 2025; Khan, et al., 2024). Chemotherapy may cause systemic side effects such as nausea, alopecia, and immune suppression, while radiotherapy can damage surrounding healthy tissue (Liu, et al., 2024; Winter, et al., 2024). Therefore, the exploration of natural sources remains important for developing safer and more effective anticancer agents.

Rhodomyrtus tomentosa (Aiton) Hassk.) locally known as Karamunting is a plant that has traditionally been used in medicine and is known to contain various secondary metabolites, such as flavonoids, tannins, terpenoids, and other phenolic compounds (Oktaviyanti, et al., 2024). Several studies have reported that metabolites from *R. tomentosa* exhibit biological activities, including antioxidant, anti-inflammatory, and anticancer properties (Idris, et al., 2022, 2023). One of its main compounds, rhodomyrtone, has been reported to have antimetastatic effects through the inhibition of cancer cell migration involving the matrix metalloproteinase (MMP) regulatory pathway (Tayeh & Watanapokasin, 2020). In addition, phenolic compounds from this plant also have the potential to influence the apoptotic mechanisms in cancer cells (Islam, et al., 2019). Although these studies demonstrate promising anticancer potential, most previous research has focused on testing cytotoxic activity or other

general mechanism without identifying specific molecular targets. Investigation examining in the interactions of *R. tomentosa* metabolites with cancer-related enzymes are still limited.

Modern cancer therapy emphasizes specific and selective molecular-targeted approaches. One important biological target is the ribonucleotide reductase (RNR) enzyme, which plays a crucial role in the synthesis of deoxyribonucleotides (dNTPs), the main precursors in DNA formation (Jung, et al., 2022). High RNR activity has been observed in various types of cancer cells due to the increased need for DNA replication during cell proliferation (G. Chen, et al., 2019). Therefore, RNR inhibition is a promising therapeutic strategy in the development of anticancer drugs. Several chemotherapeutic agents that have been used clinically, such as gemcitabine, exert their effects by inhibiting RNR activity (Huff, et al., 2022).

Advancements in computational technology have led to the widespread use of *in silico* approaches such as molecular docking, which are widely used in the early stages of drug discovery to predict ligand-receptor interactions, biological activity, and the potential toxicity of a compound before experimental testing (Paggi, et al., 2024). Molecular docking enables the identification of compounds with high binding affinity to target proteins based on binding energy values, where lower energy values indicate stronger affinity between the ligand and receptor (Pagadala, et al., 2017). This approach can also be combined with computational toxicity prediction to select compound candidates that are not only potentially active but also relatively safe. RNR has been shown to be an anticancer target, but no comprehensive study has systematically evaluated the potential of *R. tomentosa* metabolites to inhibit this enzyme. To our knowledge, specific investigations of this enzyme as a target remain limited, representing a critical gap in elucidating the molecular mechanisms underlying its anticancer activity. Moreover, studies that simultaneously integrate molecular docking analysis with

comprehensive absorption, distribution, metabolism, excretion, toxicity (ADMET) prediction to evaluate the efficacy and safety of *R. tomentosa* metabolites have not yet been conducted.

Based on this background, this study aims to evaluate the anticancer potential of active metabolites from the *R. tomentosa* plant through an *in silico* approach targeting the RNR enzyme. The analysis was performed using molecular docking with Molegro Virtual Docker (MVD) version 7.0 software to predict ligand binding affinity to the receptor, as well as pharmacokinetic and toxicity (ADMET) prediction using the ADMETlab 3.0 platform (Fu et al., 2024), as an initial stage of computational drug discovery. The results of this study are expected to provide a scientific basis for the development of natural product-based anticancer agents candidates that have the potential to be further tested through *in vitro* and *in vivo* studies.

Methods

Materials

This study was conducted using a personal computer equipped with an Intel® Core™ i3-1215U processor specifications, 8 GB RAM, and Windows 11 operating system. Molecular docking simulations were performed using Molegro Virtual Docker (MVD) version 7.0, while ligand structure construction and geometry optimization were carried out using Chem3D version 16.0. Visualization and analysis of ligand-receptor interactions were conducted using BIOVIA Discovery Studio Visualizer.

The 3D structure of target protein, RNR enzyme with PDB ID: 2WGH (Fairman et al., 2011), was obtained from the Protein Data Bank (https://www.rcsb.org). The chemical structures of the ligands were obtained from the PubChem database (https://pubchem.ncbi.nlm.nih.gov) in Simplified Molecular Input Line Entry System (SMILES) format.

Ligand Selection and Preparation

Active metabolite compounds from *R. tomentosa* plants were identified through literature searches of research articles and review papers indexed in major scientific databases, including PubMed, Scopus, Elsevier, and Google Scholar. A literature search was conducted using keywords such as '*Rhodomyrtus tomentosa'*, 'Secondary Metabolites', 'Phytochemicals', 'Bioactive Compounds', and 'Natural Products' to identify compounds that have been previously reported from this species. Compounds documented from different plant parts, including leaves, stems, flowers, fruit, and bark, were compiled as candidate ligands for further analysis.

The chemical structures of selected compounds were retrieved from PubChem in SMILES format. These structures were converted into 2D structures and subsequently were converted into 3D conformations using Chem3D version 16.0. Molecular geometry optimization was performed using the Merck Molecular Force Field (MMFF94) method until a conformation with the lowest energy was achieved. The optimized ligand structures were then exported in .mol2 file format for subsequent docking analysis (Kesuma, et al., 2022). In addition, gemcitabine was included as a reference compound due to its established role as a RNR inhibitor.

Protein Preparation

The crystal structure of the RNR enzyme was imported into MVD version 7.0 for receptor preparation. Initially, before the docking process, all water molecules, ions and non-essential co crystallized ligands were removed from the protein structure to reduce potential interference with ligand binding analysis. Subsequently, the cavity detection was performed automatically by the software to identify the potential active site regions of the protein that could serve as ligand binding site.

Docking Method Validation

The docking method was validated by performing a re-docking procedure of the native ligand present in the crystal structure of the RNR protein, namely *2′-deoxyadenosine 5′-triphosphate* (DTP). The grid parameters were defined with a resolution of 0.30 Å and a radius of 8 Å, while the grid box dimensions along the X, Y, and Z axes were adjusted according to the coordinates of the identified active site.

The accuracy of the re-docking process was evaluated by calculating the Root Mean Square Deviation (RMSD) between the predicted ligand pose and the crystal ligand orientation. The docking protocol was considered valid when the RMSD value was ≤ 2.0 Å, which indicates that the orientation of the docked ligand was similar to that of the reference structure (Pagadala, et al., 2017).

Molecular Docking Protocol

Molecular docking simulations were performed on all active metabolites of *R. tomentosa* and the reference compound gemcitabine against the RNR enzyme target using MVD version 7.0. During the simulations, ligands were treated as flexible molecules, whereas the receptor structure was maintained in a rigid conformation. The docking procedure was carried out using the docking wizard feature with standard software parameters.

Each docking simulation process was conducted in 10 independent runs to generate multiple possible binding poses, and the entire procedure was performed in three replicates to ensure the consistency and reproducibility of the results. Binding affinity was evaluated based on the MolDock Score, where more negative values indicate stronger predicted interactions between the ligand and the receptor.

Bond Energy and Molecular Interaction Analysis

The docking results were analyzed by comparing the MolDock Score of each ligand to the native ligand and the reference compounds. Ligands exhibiting lower (more negative) binding energy values were predicted to have a higher binding affinity toward the RNR enzyme. Visualization of ligand-receptor interactions was carried our using BIOVIA Discovery Studio Visualizer to identify the types of interactions formed, including hydrogen bonds, hydrophobic interactions, and steric interactions, as well as the specific amino acid residues involved in the ligand binding.

ADMET Prediction

Compound toxicity prediction was performed using the ADMETlab 3.0 online platform (https://admetlab3.scbdd/). The analysis included evaluation of Lipinski's Rule of Five, ADMET (Absorption, Distribution, Metabolism, Excretion, Toxicity) and other relevant pharmacokinetic parameters. These predictions were used to assess the drug-likeness and pharmacokinetic suitability of the compounds. The toxicity prediction results were used as a basis for selecting candidate compounds that have potential anticancer activity and favorable safety profile.

Results

Ligand Preparation

A total of 25 active metabolite compounds derived from various parts of the *R. tomentosa* plant (leaves, stems, flowers, fruits, and bark) were compiled based on a literature search, as presented in Table 1. These compounds represent various groups of secondary plant metabolite compounds, including phenolic, flavonoid, terpenoid, lipid, and tannin groups. All ligands were successfully converted into three-dimensional (3D) structures and subsequently

optimized using the MMFF94 force field to obtain minimum-energy conformations prior to molecular docking analysis. The 2D visualization of the optimized ligand structures is presented in Figure 1.

Table 1. List of Active Metabolites in *R. tomentosa*

No Compound	Compounds Name	Classification	Source	Ref
1	Delphinidin-3-Galactoside	Flavonoid (Anthocyanin)	Flowers	(Vo & Ngo, 2019)
2	Stigmast-4-en-3-one	Phytosterol	Stems	(Vo & Ngo, 2019)
3	Rhodomyrtosone B	Phenolics (Acylphloroglucinol)	Leaves, Fruits	(Idris et al., 2023)
4	Cyanidin-3-galactoside	Flavonoid (Anthocyanin)	Flowers	(Vo & Ngo, 2019)
5	Rhodomyrtosone A	Phenolics (Acylphloroglucinol)	Leaves	(Idris et al., 2023)
6	Rhodomyrtone	Phenolics (Acylphloroglucinol)	Leaves	(Idris et al., 2023)
7	Rhodomyrtosone I	Phenolics (Acylphloroglucinol)	Stems	(Idris et al., 2023)
8	Tomentosin	Phenolics (Acylphloroglucinol)	Leaves	(Marwati et al., 2025)
9	3-O-methylellagicacid	Phenolics (Ellagic acid derivative)	Stems	(Vo & Ngo, 2019)
10	Malvidin-3-glucoside	Flavonoid (Anthocyanin)	Flowers	(Vo & Ngo, 2019)
11	Rhodomyrtosone D	Phenolics (Acylphloroglucinol)	Leaves	(Idris et al., 2023)
12	Rhodomyrtosone C	Phenolics (Acylphloroglucinol)	Leaves	(Idris et al., 2023)
13	Combretol	Flavonoid	Stems	(Dachriyanus et al., 2004)
14	Afrormosin	Flavonoid (Isoflavone)	Leaves	(Hadi & Nastiti, 2023)
15	Watsonianone A	Phenolics (β-triketone)	Fruits	(Zhuang et al., 2017)
16	Aromadendrene	Terpenoid	Leaves	(Vo & Ngo, 2019)
17	Lupeol	Terpenoid	Leaves	(D. Chen et al., 2017)
18	Oleanolic acid	Terpenoid	Stems	(Fujiati et al., 2022)
19	Methyl gallate	Phenolics (Gallic acid derivate)	Stems	(Vo & Ngo, 2019)
20	B-amyrenonol	Terpenoid	Leaves	(D. Chen et al., 2017)
21	B-amyrin	Terpenoid	Leaves	(D. Chen et al., 2017)

22	A-pinene	Terpenoid	Leaves	(Vo & Ngo, 2019)
23	B-pinene	Terpenoid	Leaves	(Vo & Ngo, 2019)
24	4-O-Rhamnopyranoside	Phenolics glycoside	Stems	(Vo & Ngo, 2019)
25	Pedunculagin	Tannin (Ellagitannin)	Leaves	(Vo & Ngo, 2019)

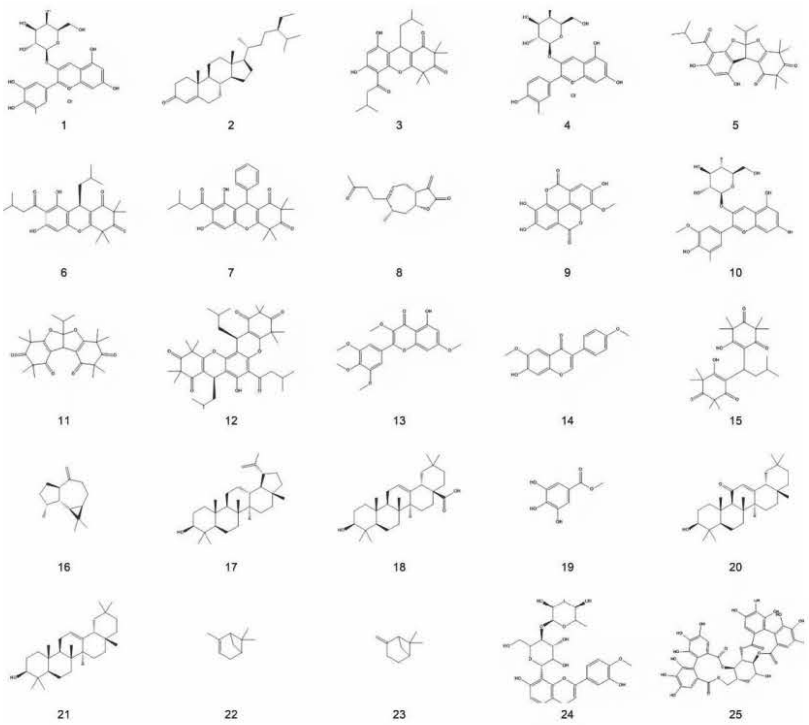

Figure 1. Two-Dimensional (2D) Structures of the 25 Selected Ligands from *R. tomentosa*. The compound names correspond to those listed in Table 1.

Docking Method Validation

Docking method validation was performed by re-docking the native ligand DTP into the active site of the RNR enzyme. The re-docking using a grid center at (X=50.49, Y=-0.42, Z=7.93) produced an RMSD value of 0.63308 Å, which is below the commonly accepted threshold (≤ 2.0 Å), as shown in Figure 2. This RMSD value indicates that the orientation and

position of the docked ligand are highly consistent with those observed in the crystal structure, thereby demonstrating the reliability of the docking protocol used and its suitability for subsequent evaluation of the test compounds.

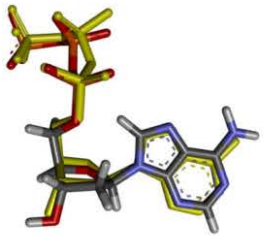

Figure 2. Re-docking Validation of the Native Ligand (DTP), showing before (yellow) and after (grey)

Bond Energy Analysis of Docking Results

The results of molecular docking simulations between the active metabolites of *R. tomentosa* and the RNR enzyme are presented in Table 2, which shows the MolDock Score values for each ligand. A more negative MolDock Score indicates a stronger binding affinity between the ligand and the receptor (Thomsen & Christensen, 2006). As a comparison, the conventional anticancer compound gemcitabine (GCQ) was used. The five compounds with the lowest MolDock Scores were Rhodomyrtosone B (−137.144 kcal/mol), Malvidin-3-glucoside (−135.173 kcal/mol), Delphinidin-3-galactoside (−132.359 kcal/mol), Rhodomyrtosone I (−130.004 kcal/mol), and Cyanidin-3-galactoside (−127.741 kcal/mol). Overall, a total of 22 compounds showed lower MolDock Score values than the reference compound gemcitabine. These values were lower than gemcitabine (−60.103 kcal/mol).

Table 2. Binding Energy Between Ligands and Receptors (Ordered from Lowest to Highest Binding Energy)

Compound No	MolDock Score			Mean ± SD (kcal/mol)
	Run 1	Run 2	Run 3	
*DTP	-183.755	-180.831	-181.419	-182.001 ± 1.547
3	-147.749	-131.069	-132.615	-137.144 ± 9.216

10	-134.269	-139.453	-131.799	-135.174 ± 3.906
1	-133.250	-133.200	-130.628	-132.359 ± 1.500
7	-134.618	-131.276	-124.118	-130.004 ± 5.364
4	-128.137	-126.376	-128.712	-127.742 ± 1.217
13	-130.925	-122.993	-116.465	-123.461 ± 7.241
2	-120.072	-120.056	-114.362	-118.163 ± 3.292
6	-114.319	-109.419	-122.351	-115.363 ± 6.529
9	-112.678	-118.215	-113.665	-114.853 ± 2.953
17	-97.974	-113.144	-99.339	-103.486 ± 8.392
14	-103.01	-100.783	-100.422	-101.405 ± 1.402
11	-90.295	-112.747	-100.261	-101.101± 11.250
8	-96.016	-102.003	-102.453	-100.157 ± 3.594
18	-91.999	-92.700	-94.315	-93.005 ± 1.188
5	-94.522	92.955	-90.245	-92.574 ± 2.164
20	-94.021	-90.173	-89.870	-91.355 ± 2.314
21	-88.489	-93.430	-89.122	-90.347 ± 2.689
12	-88.801	-80.769	-88.732	-86.100 ± 4.617
16	-85.819	-82.870	-82.849	-83.846 ± 1.709
15	-85.594	-86.125	-79.132	-83.617 ± 3.893
19	-73.638	-72.989	-68.563	-71.730 ± 2.762
24	-64.726	-68.454	-62.726	-65.302 ± 2.907
**GCQ	-61.881	-60.047	-58.381	-60.103 ± 1.751
22	-52.505	-52.365	-52.164	-52.345 ± 0.171
23	-54.379	-48.697	-47.611	-50.229 ± 3.635
25	614.347	280.012	-53.951	280.136 ± 334.149

*DTP is a native ligand; **GCQ is a reference compound

Notably, Pedunculagin (compound 25) exhibited relatively high variability in docking results, as reflected by its standard deviation (± 334.149), indicating inconsistent binding poses across replicates. Numerous unfavorable donor-donor interactions and unfavorable bumps are observed (Figure 3F), resulting in a positive average MolDock Score. A large deviation suggests that the ligand does not adopt a stable conformation within the RNR active site. This

behavior may be attributed to the structural characteristics of Pedunculagin, which belongs to the ellagitannin class and possesses a large molecular size, high polarity, and multiple rotatable bonds. These features can lead to steric hindrance and conformational flexibility, making it difficult for the ligand to fit optimally into the relatively confined binding pocket. Consequently, the docking algorithm may generate multiple energetically diverse poses, resulting in high variability.

Ligand–Receptor Interaction Analysis

Molecular interaction analysis was conducted to identify the amino acid residues involved in ligand binding at the active site of the RNR enzyme. The corresponding 2D interaction visualizations are presented in Figure 3.

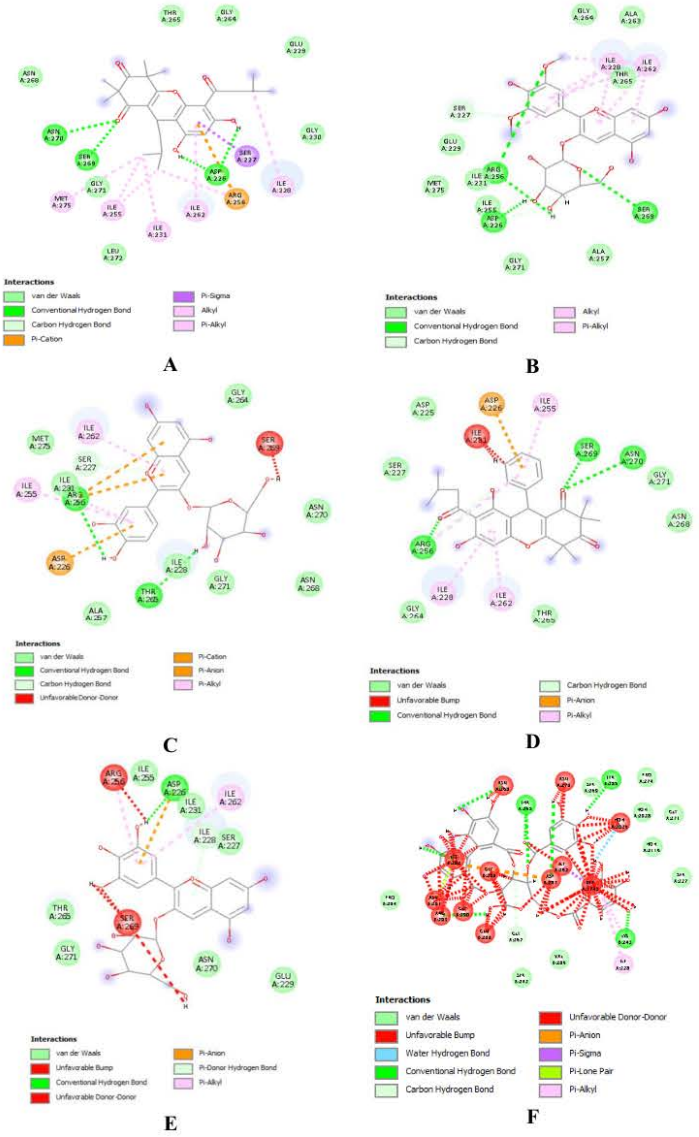
Interactions
van der Waals
Conventional Hydrogen Bond
Carbon Hydrogen Bond
Pi-Cation
Pi-Sigma
Alkyl
Pi-Alkyl
A
Interactions
van der Waals
Conventional Hydrogen Bond
Carbon Hydrogen Bond
Alkyl
Pi-Alkyl
B
Interactions
van der Waals
Conventional Hydrogen Bond
Carbon Hydrogen Bond
Unfavorable Donor-Donor
Pi-Cation
Pi-Anion
Pi-Alkyl
C
Interactions
van der Waals
Unfavorable Bump
Conventional Hydrogen Bond
Carbon Hydrogen Bond
Pi-Anion
Pi-Alkyl
D
Interactions
van der Waals
Unfavorable Bump
Conventional Hydrogen Bond
Unfavorable Donor-Donor
Pi-Anion
Pi-Donor Hydrogen Bond
Pi-Alkyl
E
Interactions
van der Waals
Unfavorable Bump
Water Hydrogen Bond
Conventional Hydrogen Bond
Carbon Hydrogen Bond
Unfavorable Donor-Donor
Pi-Anion
Pi-Sigma
Pi-Lone Pair
Pi-Alkyl
F

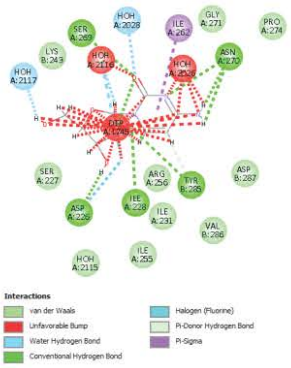

G

Figure 3. Two-dimensional (2D) interaction profiles between ribonucleotide reductase (RNR; PDB ID: 2WGH) and selected ligands. A. Rhodomyrtosone B, B. Malvidin-3-glucoside, C. Delphinidin-3-galactoside, D. Rhodomyrtosone I, E. Cyanidin-3-galactoside. F. Pedunculagin, G. Gemcitabine

Based on the re-docking results of the native ligand DTP exhibited a MolDock score of -182.001, indicating a very strong binding affinity for the target protein. The interactions formed involve various types of forces, namely hydrogen bonds with residues Asp287, Asp266, Ala263, Arg256, Gly264, Lys243, and Ile228; electrostatic interactions with Arg256 and Lys243; and steric interactions with Asp287, Asp263, Ala263, Arg256, Gly264, Lys243, and Ile288.

The reference compound gemcitabine also demonstrated multiple interaction within the active site of RNR. The 2D interaction analysis revealed that the ligand forms multiple conventional hydrogen bonds with key active site residues, including Arg256, Asp226, Tyr285, and Asn270, indicating strong and specific binding within the catalytic pocket of RNR. In addition, several water-mediated hydrogen bonds were observed, suggesting the involvement of solvent molecules in stabilizing the ligand–protein complex. Hydrophobic interactions, including π-sigma contacts with Ile262, further contributed to ligand stabilization. However,

the presence of multiple unfavorable steric interactions indicates potential spatial constraints within the binding pocket, which may affect the overall binding efficiency.

Rhodomyrtosone B showed favorable interactions through hydrogen bonds with Asp226 and Ser269, as well as electrostatic interaction with Arg256 (π-cation). These interactions were supported by extensive hydrophobic contacts with Ile and Leu residues, suggesting a stable binding conformation within the active site.

Malvidin-3-glucoside demonstrated a strong and stable interaction profile, characterized by multiple hydrogen bonds with Arg256, Asp226, and Ser269, along with extensive hydrophobic interactions involving Ile228, Ile231, and Ile262. Additional van der Waals interactions further contributed to the stabilization of the complex, indicating that Malvidin is well positioned within the active site.

Cyanidin-3-galactoside exhibited a more diverse interaction profile, forming hydrogen bonds with Arg256 and Thr265, along with electrostatic interactions involving Arg256 (π-cation) and Asp226 (π-anion). These interactions were further supported by hydrophobic contacts with surrounding residues. The presence of electrostatic interactions suggests enhanced binding stability due to stronger interaction forces compared to hydrophobic interactions alone.

Rhodomyrtosone I also demonstrated the ability to interact with the enzyme's active site through the formation of hydrogen bonds with residues Arg256 and Ser269. π-anion interactions with Asp226 and π-alkyl hydrophobic interactions with residues Ile228, Ile255, and Ile262 also contribute to the stability of the ligand-protein complex.

Delphinidin-3-galactoside formed hydrogen bonds with Asp226 and hydrophobic interactions with Ile228 and Ile262. However, the presence of unfavorable interactions, including steric clashes and donor–donor interactions with Arg256 and Ser269, may reduce the overall stability of the ligand–receptor complex despite its ability to form favorable contacts.

ADMET Prediction

The drug-likeness properties of the selected compounds were evaluated using Lipinski's Rule of Five, which is commonly used to assess the oral bioavailability potential of small molecules. According to this rule, a compound is more likely to exhibit good absorption and permeability if it meets the following criteria: molecular weight ≤ 500 Da, logP ≤ 5, hydrogen bond donors ≤ 5, and hydrogen bond acceptors ≤ 10 (Lipinski et al., 1997).

The analysis demonstrated that two of the selected compounds complied with Lipinski's criteria, indicating favorable drug-likeness properties. However, slight deviations were observed in several compounds, particularly in terms of the number of hydrogen bond donors and acceptors, which may be attributed to the presence of multiple hydroxyl groups commonly found in phenolic compounds. **Table 3** summarizes the pharmacokinetic and toxicity profiles of the five tested compounds.

Table 3. Results of Lipinski's rule of five analysis

Compound	MW (< 500 Da)	Lipinski's Rule of Five Hydrogen Bonds		Log P	Interpretation
		Donor (< 5)	Acceptor (< 10)		
Rhodomyrtosone B	442.24	2	6	4.93	Accepted
Malvidin-3-glucoside	493.13	7	12	-0.018	Rejected
Cyanidin-3-galactoside	449.11	8	11	0.012	Rejected
Rhodomyrtosone I	462.2	2	6	4.413	Accepted
Delphinidin-3-galactoside	465.1	9	12	-0.923	Rejected

The pharmacokinetic properties encompass absorption, distribution, metabolism, and excretion (ADME), which were evaluated using two to four parameters for each category (Yuniarta et al., 2025). In the absorption analysis, parameters included Caco-2 permeability (>-5.15 log cm/s) and human intestinal absorption (HIA), both of which serve as indicators of oral bioavailability. Additionally, the assessment of P-glycoprotein (P-gp) inhibitor and

substrate properties (ranging from 0 to 0.3) was performed to determine the potential for efflux-mediated drug resistance.

Table 4. Pharmacokinetic and toxicity prediction.

	Compounds				
	Rhodomyrtosone B	**Malvidin-3-glucoside**	**Cyanidin-3-galactoside**	**Rhodomyrtosone I**	**Delphinidin-3-galactoside**
Absorption					
Caco-2 Permeability (Log cm/s)	-4.876	-6.151	-6.443	-4.922	-6.46
Pgp-Inhibitor	+	---	---	+++	---
Pgp-Substrate	---	-	+	---	+
HIA	---	--	---	---	---
Distribution					
PBB (%)	91.4 %	85.9 %	84.3 %	96.5%	82.2%
VDss (L/kg)	0.488	-0.217	-0.021	1.268	0.028
BBB Penetration	--	---	---	---	---
Fu (%)	9.0 %	13.1 %	16.2 %	2.5%	17.7%
Metabolism					
CYP2C19 Inhibitor	+++	---	---	++	---
CYP2C19 Substrate	+++	---	---	+++	---
CYP3A4 Inhibitor	+++	---	---	+++	---
CYP3A4 Substrate	+++	---	---	+++	---
Excretion					
$T_{1/2}$	1.095	4.092	3.959	0.603	4.107
Toxicity					
AMES	0.424	0.997	0.995	0.31	0.994
Carcinogenesis	0.518	1.0	1.0	0.351	1.0
H-HT	0.71	0.905	0.983	0.644	0.001
Skin Sensitization	0.564	1.0	1.0	0.546	0.373
LD_{50}	0.552	0.048	0.024	0.593	0.406

HIA: human intestinal absorption; Pgp-inhibitor and substrate: P-glycoprotein inhibitor and substrate; PPB: plasma protein binding; VDss: Volume of distribution at steady state; BBB: Blood-brain Barrier; Fu: Fraction unbound in plasma; T1/2: the half-life; H-HT: human hepatotoxicity; The prediction probability values are transformed into six symbols: 0-0.1(---), 0.1-0.3(--), 0.3-0.5(-), 0.5-0.7(+), 0.7-0.9(++), and 0.9-1.0 (+++).

Discussion

This study evaluated the potential of metabolites from *Rhodomyrtus tomentosa* as inhibitors of the RNR enzyme using molecular docking and ADMET prediction. Before molecular docking was performed, a validation step was first conducted to ensure that the

applied protocol could reliably reproduce the binding pose of the ligand within the active site of the receptor. The docking method was validated by re-docking the native ligand DTP into the crystal structure of the RNR enzyme. This procedure was carried out to evaluate the robustness of the docking protocol in predicting ligand–receptor interactions and estimating the binding affinity of the compound toward the target protein (Nivatya, et al., 2025; Sarmoko, et al., 2025).

Validation of the docking method through re-docking of the original DTP ligand into the active site of the RNR enzyme produced an RMSD value of 0.63308 Å, indicating a good level of accuracy and reproducibility of the docking protocol employed in this study. An RMSD value below 2.0 Å is generally accepted as evidence that the orientation and position of the docked ligand are highly compatible with the crystal structure of the protein, thereby supporting the reliability of the in silico approach for evaluating the binding affinity of the selected compound to the RNR target. In this study, the low RMSD value further confirms the appropriateness of the selected docking parameters and demonstrates the robustness of the method. It also suggests that the defined binding cavity appropriately represents the biologically relevant active site of RNR (Vittorio, et al., 2024).

Molecular docking results show that all selected compounds had negative binding energy values, indicating favorable interactions with the target protein. The native ligand DTP exhibited the lowest binding energy, which reflects its role as the natural substrate of the enzyme and confirms its optimal structural compatibility with the active site (Pagadala et al., 2017. These findings highlight the potential of *R. tomentosa* as a source of bioactive compounds capable of interacting with key molecular targets in cancer cell proliferation. The in silico approach, particularly molecular docking, has been widely used as an initial strategy in identifying inhibitor candidates against oncogenic targets, including RNR. Additionally, previous reports on the ability of *R. tomentosa* active metabolites to interact with other

molecular targets, such as the Smoothened (SMO) receptor (Marwati, et al., 2025), further support the multitarget pharmacological potential of this plant. This multitarget mechanism may offer therapeutic advantages in overcoming the anticancer drug resistance problems that often arise from single-target chemotherapy.

Among all test compounds, the five compounds with the lowest MolDock Scores were Rhodomyrtosone B (−137.144 kcal/mol), Malvidin-3-glucoside (−135.173 kcal/mol), Delphinidin-3-galactoside (−132.359 kcal/mol), Rhodomyrtosone I (−130.004 kcal/mol), and Cyanidin-3-galactoside (−127.741 kcal/mol), indicating favorable binding affinities toward the RNR active site. These values were lower than that of gemcitabine (-60.103 kcal/mol).

The docking results demonstrated that tested compounds exhibited stronger binding affinity than Gemcitabine, as reflected by their lower MolDock scores. Among them, Rhodomyrtosone B showed the most favorable interaction with an average MolDock score, followed by Malvidin-3-glucoside and Delphinidin-3-galactoside. This difference may be attributed to the structural compatibility of the tested compounds with the active site of RNR. The polyphenolic structures of these compounds, which are rich in hydroxyl groups, enable the formation of multiple hydrogen bonds with key residues such as Arg256, Asp226, and Tyr285, thereby enhancing binding stability (Shahidi & Dissanayaka, 2023). Additionally, these compounds generally exhibited fewer unfavorable steric interactions, indicating a more optimal binding conformation within the binding pocket.

In contrast, gemcitabine showed several unfavorable interactions, indicating a less optimal binding conformation in this docking model. This observation may be related to the fact that gemcitabine acts as a prodrug, requiring intracellular phosphorylation into its active diphosphate and triphosphate forms to effectively inhibit the enzyme. Since the docking study was performed using the parent structure, the observed binding affinity may underestimate its actual biological activity.

Ligand–receptor interaction analysis further demonstrated that these compounds engaged in various combinations of hydrogen bonds and hydrophobic interactions with key active-site residues, including Arg256, Asp226, and Ser269. These residues were consistently involved in hydrogen bonding and electrostatic interactions, indicating their crucial role in ligand stabilization and recognition. In addition, hydrophobic residues including Ile228, Ile231, and Ile262 contributed to ligand stabilization by providing a nonpolar environment within the binding pocket. The combination of hydrogen bonding, electrostatic, and hydrophobic interactions plays a critical role in maintaining the stability of the ligand–receptor complex.

Among the evaluated compounds, Rhodomyrtosone B and Malvidin-3-glucoside exhibited the most favorable interaction profiles, characterized by stable hydrogen bonding, electrostatic interactions, and extensive hydrophobic interactions, suggesting strong binding stability. Cyanidin-3-galactoside and Rhodomyrtosone I also showed favorable interactions, although with slightly less optimal binding patterns. In contrast, Delphinidin-3-galactoside exhibited several unfavorable interactions, which may reduce the overall stability of the complex despite having relatively good binding affinity. The presence of electrostatic interactions in Cyanidin-3-galactoside and Rhodomyrtosone B further enhances binding stability, as these interactions are generally stronger and more specific. Compared with DTP, which shows similar amino acid interactions to those observed in the selected compounds, the broader interaction profiles observed in these compounds indicate more stable ligand–receptor complex formation, consistent with their lower MolDock Scores. The presence of multiple hydrogen bonds combined with hydrophobic interactions may synergistically stabilize ligand binding within the catalytic cavity, as reported in previous docking-based studies (Lai et al., 2024).

Biologically, RNR is a key enzyme in the synthesis of deoxyribonucleotides (dNTPs) required for DNA replication and repair. Increased RNR activity in cancer cells makes it a strategic target in anticancer therapy. The strong interaction of *R. tomentosa* compounds with important residues on the active site of RNR suggests that these compounds have the potential to inhibit the catalytic activity of the enzyme, thereby disrupting dNTP availability and suppressing cancer cell proliferation. Although the specific inhibition mechanism cannot be confirmed based solely on docking results, the high binding affinity provides promising initial indications regarding the potential of both compounds as RNR inhibitors. Because these compounds bind in the active site of the enzyme, they may act as competitive inhibitor by competing with the natural substrate for binding to the catalytic cavity (Pesaresi, 2023). However, further enzymatic assays is needed to confirm this mechanism.

In addition to binding affinity, pharmacokinetic properties are crucial factors in drug candidate selection, were further evaluated using ADMET prediction. In terms of absorption, all compounds exhibited low Caco-2 permeability and low human intestinal absorption (HIA), indicating limited oral bioavailability. This may be attributed to the high polarity of the compounds, particularly due to the presence of multiple hydroxyl groups, which can hinder passive diffusion across biological membranes. Additionally, some compounds were predicted to interact with P-glycoprotein (P-gp), either as inhibitors or substrates, suggesting that efflux mechanisms may influence their absorption and intracellular concentration.

Toxicity prediction results show that, among the five compounds with the best binding energy values, several exhibited potential toxicity, especially anthocyanin compound, Malvidin-3-glucoside, Delphinidin-3-galactoside and Cyanidin-3-galactoside. Therefore, these compounds are considered less suitable and are not recommended for further development despite their strong predicted binding affinity. Conversely, Rhodomyrtosone B and Rhodomyrtosone I exhibit a relatively safer toxicity profile based on the Ames test,

carcinogenicity, hepatotoxicity, and skin sensitivity parameters compared with other metabolites evaluated in this study. The relatively higher LD_{50} values of these two compounds also indicate a lower level of predicted acute toxicity compared to several other metabolites. These findings demonstrate that strong molecular interactions alone do not necessarily translate into pharmacological suitability, emphasizing the importance of early-stage safety evaluation in computational drug discovery.

The integration of molecular docking results and toxicity predictions confirms that the selection of candidate compounds cannot be based solely on binding affinity values for molecular targets but must also consider the balance between biological activity potential and pharmacological safety. Based on this integrative approach, Rhodomyrtosone B and Rhodomyrtosone I emerged as the most rational candidates for further development as natural-based anticancer agents targeting the RNR enzyme. These findings provide a strong scientific basis for further research through in vitro and in vivo experimental testing to confirm their biological activity and inhibition mechanism in greater depth. Nevertheless, this study employed a rigid receptor model and static docking simulations, which may not fully capture the protein flexibility and dynamic conformational changes. Therefore, further studies incorporating molecular dynamics simulations and experimental activity testing are necessary to obtain more comprehensive and reliable predictions.

Conclusion

Based on the molecular docking analysis targeting the RNR enzyme, the active metabolites of *R. tomentosa* demonstrated variable binding affinities toward the molecular target. Rhodomyrtosone B and Rhodomyrtosone I emerged as the most favorable candidate, exhibiting the strongest binding affinity among the tested metabolites and a relatively balanced pharmacokinetic and toxicity profile. Ligand–receptor interaction analysis showed the

involvement of key active-site residues, supporting the stability of the ligan–protein complex. ADMET prediction results using the ADMETlab 3.0 platform show that Rhodomyrtosone B and Rhodomyrtosone I also have relatively safer in silico toxicity profiles based on Ames test parameters, carcinogenicity, hepatotoxicity, skin sensitivity, and acute LD_{50} values. By integrating binding affinity with predicted toxicity profiles, both compounds emerge as promising lead candidates for natural-based anticancer agents targeting the RNR enzyme. However, these findings remain predictive in nature and require further validation through comprehensive in vitro and in vivo testing studies to confirm their biological activity and mechanism of inhibition.

Acknowledgment

The authors would like to express their sincere gratitude to the University of Surabaya for providing financial support through the Internal Research Grant Scheme (Basic Research Program). This funding support was instrumental in facilitating the successful completion of this study.

References

Chen, D., Xu, F., Zhang1, P., Deng, J., Sun, H., Wen, X. and Liu, J., 2017, Practical synthesis of a-Amyrin, b-Amyrin, and lupeol: The potential natural inhibitors of human oxidosqualene cyclase, ARCH PHARM Archiv Der Pharmazie, **350**(12), 1–9.

Chen, G., Luo, Y., Warncke, K., Sun, Y., Yu, D.S., Fu, H., Behera, M., Ramalingam, S.S., Doetsch, P.W., Duong, D.M., Lammers, M., Curran, W.J. and Deng, X., 2019, Acetylation regulates ribonucleotide reductase activity and cancer cell growth, Nature Communications, **10**, 3213.

Dachriyanus, Fahmi, R., Sargent, M.V., Skeltonc, B.W. and White, A.H., 2004, 5-Hydroxy-3,3000,4000,5000,7-pentamethoxyflavone (combretol), Acta Crystallographica Section E, **60**(1), 86–88.

Fairman, J. W., Wijerathna, S. R., Ahmad, M. F., Xu, H., Nakano, R., Jha, S., Prendergast, J., Welin, R. M., Flodin, S., Roos, A., Nordlund, P., Li, Z., Walz, T., & Dealwis, C. G., 2011, Structural basis for allosteric regulation of human ribonucleotide reductase by nucleotide-induced oligomerization, Nature Structural and Molecular Biology, **18**(3), 316–322.

Ferlay, J., Rebecca, M.E. and Mph, L.S., 2024, Global cancer statistics 2022: GLOBOCAN estimates of incidence and mortality worldwide for 36 cancers in 185 countries, International Agency for Research on Cancer/World Health Organization, **74**(3), 229–263.

Fu, L., Shi, S., Yi, J., Wang, N., He, Y., Wu, Z., Peng, J., Deng, Y., Wang, W., Wu, C., Lyu, A., Zeng X., Zhao W., Hou, T., and Cao, D., 2024. ADMETlab 3.0: an updated comprehensive online ADMET prediction platform enhanced with broader coverage, improved performance, API functionality and decision support, Nucleic Acid Research, 52(W1), W422-W431.

Fujiati, F., Haryati, H., Joharman, J. and Utami, S.W., 2022, In vitro metabolite profiling and anti-inflammatory activities of Rhodomyrtus tomentosa with red blood cell membrane stabilization methods, Reports of Biochemistry & Molecular Biology, **11**(3), 503–510.

Gu, Y., Yang, R., Zhang, Y., Guo, M., Takehiro, K. and Zhan, M., 2025, Molecular mechanisms and therapeutic strategies in overcoming chemotherapy resistance in cancer, Molecular Biomedicine, **6**(2), 2–22.

Hadi, S. and Nastiti, K., 2023, Activity predication of Rhodomyrtus tomentosa (Aiton) Hassk against ACE1 inhibitors, Science Midwifery, **11**(2), 348–355.

Huff, S.E., Winter, J.M. and Dealwis, C.G., 2022, Inhibitors of the cancer target ribonucleotide reductase, past and present, MDPI Biomolecules, **12**(6), 815.

Idris, M., Purnomo, A.S., Martak, F., Kim, Y. and Fatmawati, S., 2023, Chemical compounds and pharmaceutical properties of Rhodomyrtus tomentosa: A traditional medicinal herb from South Kalimantan, Indonesia, Journal of Hunan University (Natural Sciences), **50**(8), 100–123.

Idris, M., Sukandar, E.R., Purnomo, A.S., Martak, F. and Fatmawati, S., 2022, Antidiabetic, cytotoxic and antioxidant activities of Rhodomyrtus tomentosa leaf extracts, RSC Advances, **12**(39), 25697–25710.

Islam, O., Bacchetti, T. and Ferretti, G., 2019, Alterations of antioxidant enzymes and biomarkers of nitro-oxidative stress in tissues of bladder cancer, Hindawi Oxidative Medicine and Cellular Longevity, **2019**(1), 10.

Jung, K., Kwon, S., Jung, J. and Bahn, Y.-S., 2022, Essential roles of ribonucleotide reductases under DNA damage and replication stresses in Cryptococcus neoformans, Microbiology Spectrum, **10**(4), 1–13.

Kesuma, D., Yuniarta, T.A., Putra, G.S., Sumari, S., Sulistyowaty, M.I. and Anwari, F., 2022, In silico, synthesis, structure elucidation and anticancer activity study of 2-(3,4-dichlorophenyl)-4H-benzo[d][1,3]oxazin-4-one, Pakistan Journal of Pharmaceutical Sciences, **35**(5), 1391–1398.

Khan, S.U., Fatima, K., Aisha, S. and Malik, F., 2024, Unveiling the mechanisms and challenges of cancer drug resistance, Cell Communication and Signaling, **22**(109), 1–26.

Lai, H., Wang, L., Qian, R., Huang, J., Zhou, P., Ye, G., Wu, F., Wu, F., Zeng, X., Liu, W., 2024, Interformer: an interaction-aware model for protein-ligand docking and affinity prediction, Nature Communications, **15**, 10223.

Lipinski, C.A., Lombardo, F., Dominy, B.W., and Feeney, P.J., 1997, Experimental and computational approaches to estimate solubility and permeability in drug discovery and development settings, Advanced Drug Delivery Reviews, **23**(1-3), 3-25.

Liu, B., Zhou, H., Tan, L., Siu, K.T.H. and Guan, X.-Y., 2024, Exploring treatment options in cancer: Tumor treatment strategies, Signal Transduction and Targeted Therapy, **9**(175), 1–44.

Marwati, M., Alam, G., Yulianty, R., Sami, F.J. and Nur, S., 2025, In silico evaluation of the glioma activity of reported compounds from the extract Rhodomyrtus tomentosa (Aiton) Hassk., Jurnal Penelitian Pendidikan IPA, **11**(6), 215–226.

Nivatya, H.K., Singh, A., Kumar, N., Sharma, L., Singh, V. and Mishra, R., 2025, Assessing molecular docking tools: Understanding drug discovery and design, Future Journal of Pharmaceutical Sciences, **11**(111), 1–31.

Oktaviyanti, N.D., Budiono, R., Fitriani, E.W. and Avanti, C., 2024, Optimization ultrasound-assisted extraction using choline chloride-based natural deep eutectic solvent to increase phenolic compounds and antioxidants from Rhodomyrtus tomentosa leaves, International Journal of Applied Pharmaceutics, **16**(5), 83–90.

Pagadala, N.S., Syed, K. and Tuszynski, J., 2017, Software for molecular docking: A review, Biophysical Reviews, **9**, 91–102.

Paggi, J.M., Pandit, A. and Dror, R.O., 2024, The art and science of molecular docking, Annual Review of Biochemistry, **93**, 389–410.

Pesaresi, A., 2023, Mixed and non-competitive enzyme inhibition: underlying mechanisms and mechanistic irrelevance of the formal two-site model, Journal of Enzyme Inhibition and Medicinal Chemistry, **38(**1), 2245168.

Sarmoko, Suprahman, N.Y., Putri, R.A., Zammi, A., Hakim, A., Cahyadi, D.R. and Saputra, M.Y., 2025, In silico analysis of Cucurbitacin IIa and Cucurbitacin IIb as potential

modulators of oxidative stress regulatory proteins, Indonesian Journal of Cancer Chemoprevention, **15**(3), 224–236.

Shahidi, F., Dissanayaka, C.S., 2023, Phenolic-protein interactions: insight from food and health perspectives, Food Production, Processing and Nutrition, **5**, 2.

Tayeh, M. and Watanapokasin, R., 2020, Antimetastatic potential of rhodomyrtone on human chondrosarcoma SW1353 cells, Evidence-Based Complementary and Alternative Medicine, **2020**(1), 12.

Thomsen, R. and Christensen, M.H., 2006, MolDock: A New Technique for High-Accuracy Molecular Docking, Journal of Medicinal Chemistry, **49**(11), 3315-3321.

Vittorio, S., Lunghini, F., Morerio, P., Gadioli, D., Orlandini, S., Silva, P., Martinovic, J., Pedretti, A., Bonanni, D., Del Bue, A., Palermo, G., Vistoli, G., Beccari, A.R., 2024, Addressing docking pose selection with structure-based deep learning: Recent advances, challenges and opportunities, Computational and Structural Biotechnology Journal, **23**, 2141–2151.

Vo, T.S. and Ngo, D.H., 2019, The health beneficial properties of Rhodomyrtus tomentosa as potential functional food, MDPI Biomolecules, **9**(2), 1–16.

Winter, R.C., Amghar, M., Wacker, A.S., Bakos, G., Ta, H. and Roscher, M., 2024, Future treatment strategies for cancer patients combining targeted alpha therapy with pillars of cancer treatment: External beam radiation therapy, checkpoint inhibition immunotherapy, cytostatic chemotherapy, and brachytherapy, MDPI Pharmaceuricals, **17**(8), 1031.

Yuniarta, T.A., Kesuma, D., Putra, P.P., 2025, Virtual Screening, ADMET Evaluation, and Molecular Docking Approach in the Discovery of Novel Potential Sweetening Agent, MPI (Media Pharmaceutica Indonesiana), **7**(2), 124-137.

Zhuang, L., Chen, L.-F., Zhang, Y.-B., Liu, Z., Xiao, X.-H., Tang, W., Wang, G.-C., Song,

W.-J., Li, Y.-L. and Li, M.-M., 2017, Watsonianone A from Rhodomyrtus tomentosa fruit attenuates respiratory-syncytial-virus-induced inflammation in vitro, Agricultural and Food Chemistry, **65**(17), 3481–3489.

IJCC

ORIGINALITY REPORT

6%	6%	6%	%
SIMILARITY INDEX	INTERNET SOURCES	PUBLICATIONS	STUDENT PAPERS

PRIMARY SOURCES

1	repository.ubaya.ac.id Internet Source	2%
2	www.frontiersin.org Internet Source	1%
3	S Shabana, Annegowda Hardur Venkatappa. "Investigation of Carissa carandas L. Phytoconstituents Targeting PARP1 for the Management of Polycystic Ovarian Syndrome Complications: An In-silico Study", Journal of Herbal Medicine, 2026 Publication	1%
4	Suvankar Karmakar, Sk Aftabul Alam, Samiran Mondal. "Naturally occurring C-C and C-O-C-linked biflavonoids as potential inhibitors of the SARS-CoV-2 main protease (Mpro)", Virology, 2026 Publication	1%
5	pubs.acs.org Internet Source	1%
6	eksakta.ppj.unp.ac.id Internet Source	1%

Exclude quotes	On	Exclude matches	< 1%
Exclude bibliography	On		

IJCC

GRADEMARK REPORT

FINAL GRADE

/0

GENERAL COMMENTS

PAGE 1

PAGE 2

PAGE 3

PAGE 4

PAGE 5

PAGE 6

PAGE 7

PAGE 8

PAGE 9

PAGE 10

PAGE 11

PAGE 12

PAGE 13

PAGE 14

PAGE 15

PAGE 16

PAGE 17

PAGE 18

PAGE 19

PAGE 20

PAGE 21

PAGE 22

PAGE 23

PAGE 24

PAGE 25

PAGE 26

PAGE 27